JPEDAV (2008) 29:488–492
DOI: 10.1007/s11669-008-9416-7
1547-7037 ©ASM International

Experimental Determination and Atomistic Simulation on the Structure of $FeZn_{13}$

Y. Liu, X.P. Su, F.C. Yin, Z. Li, and Y.H. Liu

(Submitted April 7, 2008; in revised form July 15, 2008)

By X-ray diffraction combined with Rietveld structure refinement, the crystal structure of $FeZn_{13}$ was determined experimentally in this study. The results indicated that the structure of $FeZn_{13}$ is monoclinic and the lattice parameters are a = 1.3408 nm, b = 0.7605 nm, c = 0.5074 nm, and β = 127.206°. It was confirmed that Fe atoms occupy the 2c position (0, 0, 0.5) in space group $C2/m$, and the coordinates of Zn atoms at the Zn(1) position are (0.114, 0.5, 0.293), which supports the results from Belin et al. (*Acta Cryst. C* 56:267, 2000). In addition, an atomistic calculation was carried out to determine the crystal structure based on the interatomic potentials obtained using the lattice inversion method, and Fe atoms are substituted by Zn atoms in the narrow solubility range of $FeZn_{13}$, which is the fundamental for studying the solubility and site preference of alloying elements of $FeZn_{13}$. Good agreement between the experimental results and the theoretical calculations was achieved.

Keywords atomistic simulations, crystal structure, intermetallics, X-ray diffraction (XRD)

1. Introduction

Among the four intermetallics in the Fe-Zn binary system, the ζ phase, $FeZn_{13}$, has been studied most intensively due mainly to the critical role it plays in the galvanizing of reactive steels containing Si.[1-3] The Si-containing steels experience uncontrolled attack from the molten Zn in hot-dip batch galvanizing; this results in excessively thick coatings with an unattractive gray appearance. This phenomenon is often referred to as the "Sandelin effect."[4] To explore the mechanism of this phenomenon, the investigation of solubility and site preference of alloying elements such as Si, Ni, Bi, etc. in $FeZn_{13}$ is necessary. However, the crystal structure of $FeZn_{13}$ and, in particular, the coordinates of the atoms need further clarification. Götzl et al. first determined the lattice parameters of $FeZn_{13}$ in the alloy systems (Mn, Fe, Co)-Zn and proposed that the possible space groups were $C2$, Cm, or $C2/m$.[5] Later, Brown[6] described the structure concretely and postulated the probable position for the transition metal atoms (Fe, Mn, Co). In 1979, Gellings and his collaborators characterized all Fe-Zn intermetallics including $FeZn_{13}$.[7] Their results agreed well with those of Brown.[6] However, Gellings et al. chose a different a axis with a smaller β angle, resulting in a very different set of parametric values. In 2000, Belin and his co-workers[8] re-examined the structure of $FeZn_{13}$ and showed an obviously different coordinate for the Zn atom at the 4i position. They also pointed out that Fe atoms were uniquely located at the 2c position (space group $C2/m$). The findings of previous authors were shown in Table 1 (columns 3 to 5), we can see that there is dispute about the atoms coordinates for Fe and Zn at Zn(1) sites, and the cell parameters remains difference. In the present study, to uniformly determine the lattice parameters, the atom coordinates and the atom substitution in the narrowed solubility range, the structure of $FeZn_{13}$ was determined experimentally and the results that were obtained were compared with atomistic calculations of the structure based on the interatomic potentials obtained by the lattice inversion method.[9]

Y. Liu, X.P. Su, F.C. Yin, and **Z. Li,** Key Laboratory of Materials Design and Preparation Technology of Hunan Province, School of Mechanical Engineering, Xiangtan University, Hunan, P.R. China; **Y.H. Liu,** Teck Cominco Metals Ltd., Product Technology Centre, 2380 Speakman Drive, Sheridan Science and Technology Park, Mississauga, ON, Canada L5K 1B4. Contact e-mail: sxping@xtu.edu.cn.

2. Methodology

2.1 Experimental

A sample of about 8 g of the nominal composition $FeZn_{13}$ was prepared using elemental metal sheets with purities of 99.99%. The weighted metals were sealed in an evacuated quartz tube which was heated to above the liquidus temperature and kept at 1000 °C for 12 h, then quenched in water using the special method developed by Su et al.[3] to minimize Zn loss. This special quenching method ensured that the surface of the molten alloy was kept above the water level until solidification was complete, thus allowing Zn vapor to return to the melt and minimizing the Zn loss. The sealed sample was further equilibrated at 450 °C for 45 days before regular water quenching. The crystal structure and purity of the sample were identified by analyzing their X-ray powder diffraction (XRD) patterns

Table 1 Comparison of the refined cell parameters for $FeZn_{13}$(a) with the reported data

	Experiment	Ref 5	Ref 7	Ref 6	Calculation
a, nm	1.34077(5)	1.3424	1.3394	1.0862	1.3327 (0.60%)
b, nm	0.76050(3)	0.7608	0.7598	0.7608	0.7478 (1.67%)
c, nm	0.50742(2)	0.5061	0.5066	0.5061	0.5295 (4.35%)
β	127.206(1)°	127.30°	127.23°	100.53°	129.03° (1.43%)
Zn(0)(2a)	0,0,0	0,0,0 (0,0,0.5)(b)	0,0,0		0,0,0
Fe(2c)	0,0,0.5	0,0,0.5 (0,0,0)(b)	0,0,0.5		0,0,0.5
Zn(1) (4i)	0.114,0.5,0.293	0.112,0,0.292	0.114,0.5,0.294		0.11,0.5,0.30
Zn(2) (4i)	0.219,0,0.072	0.220,0,0.073	0.220,0,0.069		0.23,0,0.08
Zn(3) (8j)	0.077,0.295,0.836	0.077,0.292,0.835	0.076,0.295,0.834		0.08,0.30,0.84
Zn(4) (8j)	0.176,0.179,0.546	0.176,0.178,0.545	0.175,0.179,0.549		0.18,0.18,0.56

(a) The data in Table 1 is referring to the centrosymmetric space group *C*2/*m*
(b) The possible atom coordinates for Zn and Fe from Ref 5

generated by a Rigaku D/max-2500 diffractometer operating at 40 kV and 200 mA with Cu-Kα radiation. The XRD signal was collected from 13° to 145° of the 2θ angle in a step-scan model with a 2θ increment of 0.02°. Rietveld analysis of the diffraction pattern was carried out to determine the crystal structure.

2.2 Lattice Inversion Technique

Many forms of empirical potential between atom pairs are difficult to implement because there are too many adjustable parameters. To completely avoid parameter adjustments, Chen et al.[10,11] obtained the cohesive energy from ab initio computations and then deduced the pair potentials using the Mobius-inversion formula in number theory. Based on the obtained pair potentials, Chen et al. have performed a theoretical study on the phase stability, site preference, and lattice parameters for $Gd(Fe,T)_{12}$,[9] $Sm(Fe,T)_{12}$,[12] and $NaZn_{13}$-type intermetallics.[13] Recently, the interatomic pair potentials were employed to investigate the stability, structural, and thermodynamic properties of transition metal carbides.[14] These indicate the validity of ab initio potentials on the structure simulation of rare-earth compound and carbides. In the present study, the properties of Fe-Zn systems were studied by atomic simulation based on the interatomic potentials which were acquired by this lattice inversion method.

The methods of obtaining the cohesive energy curves and the lattice inversion technique have been reported in detail in a previous work.[9] A brief introduction to this method is given as follows: it assumes that the total cohesive energy per atom in a perfect crystal can be written as the sum of pair potentials, i.e.,

$$E(x) = \frac{1}{2}\sum_{n=1}^{\infty} r_0(n)\phi(b_0(n)x) \qquad \text{(Eq 1)}$$

where x is the nearest-neighbor interatomic distance, $r_0(n)$ is the nth neighbor coordination number, $b_0(n)x$ is the distance between the reference central atom and its nth neighbor, and $\phi(x)$ is pair potential. By self-multiplicative process of the element in $\{b_0(n)\}$, the $\{b(n)\}$ forms a closed multiplicative semi-group. Equation 1 can be rewritten as

$$E(x) = \frac{1}{2}\sum_{n=1}^{\infty} r(n)\phi(b(n)x) \qquad \text{(Eq 2)}$$

where

$$r(n) = \begin{cases} r_0(b_0^{-1}[b(n)]), & \text{if} \quad b(n) \in \{b_0(n)\}, \\ 0 & \text{if} \quad b(n) \notin \{b_0(n)\} \end{cases} \qquad \text{(Eq 3)}$$

and the pair potential from the inversion can be expressed as

$$\phi(x) = 2\sum_{n=1}^{\infty} I(n)E(b(n)x) \qquad \text{(Eq 4)}$$

where the coefficient $I(n)$ can be obtained by

$$\sum_{b(n)/b(k)} I(n)r\left(b^{-1}\left[\frac{b(k)}{b(n)}\right]\right) = \delta_{k1} \qquad \text{(Eq 5)}$$

$I(n)$ is uniquely determined by the crystal geometrical structure, which is independent of the kind of the concrete element. Thus the interatomic pair potentials can be obtained from the known cohesive energy function $E(x)$. The important interatomic pair potential curves relevant to this study are shown in Fig. 1. These potential curves can be described by Morse function,

$$\phi(x) = D_0\{\exp[-\alpha(x/R_0 - 1)] - 2\exp[-\alpha/2(x/R_0 - 1)]\} \qquad \text{(Eq 6)}$$

where x is the distance between two atoms while D_0, α, and R_0 are potential parameters.

3. Results and Discussion

3.1 Crystal Structure of $FeZn_{13}$

The X-ray diffraction pattern obtained in the present study (Fig. 2) was indexed according to the X-ray Powder

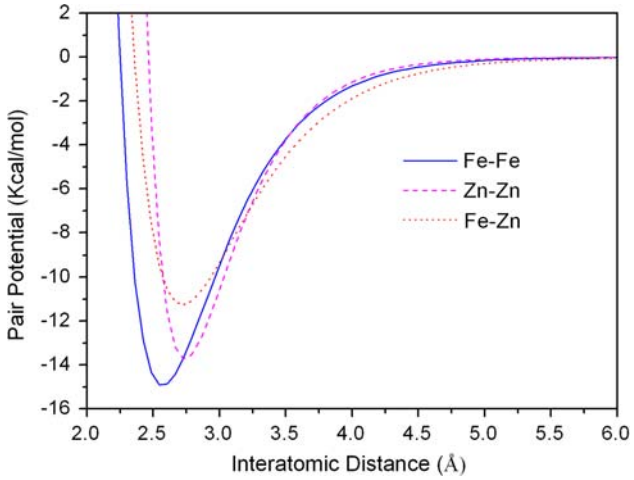

Fig. 1 Interatomic potentials for Fe-Fe, Zn-Zn, and Fe-Zn pairs

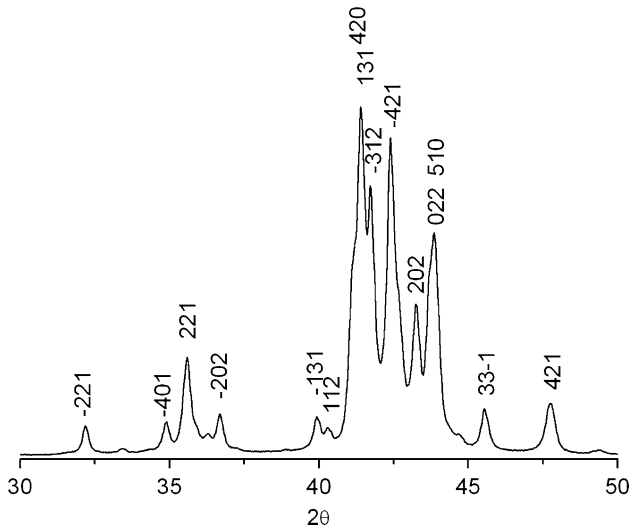

Fig. 2 X-ray diffraction pattern of the $FeZn_{13}$ crystal

Diffraction Standards published by J.C.P.D.S[15] for the ζ-$FeZn_{13}$ phase, which refers to the work performed in 1979.[7]

The Rietveld analysis of the crystal structure of $FeZn_{13}$ was performed using the computer program FULLPROF.[16] The refinement confirmed that $FeZn_{13}$ belonged to the *C*2/*m* space group. Computer simulation of the relative intensity ratio between 2θ = 16.45 and 2θ = 17.64 indicated that Fe should preferentially locate at the 2c position (0, 0, 0.5). The refined lattice parameters for $FeZn_{13}$ are a = 1.34077(5) nm, b = 0.76050(3) nm, c = 0.50742(2) nm, and β = 127.206(1)°. The schematic illustration of the lattice is shown in Fig. 3. It is clear that the Fe atom occupies the 2c position (0, 0, 0.5) at the center of an icosahedron whose 12 vertices are occupied by Zn atoms. In each unit cell, another four Zn atoms exist at the 4i positions between the icosahedra.

The lattice parameters obtained from this study are listed in Table 1 (column 2) together with the data reported in the literature (columns 3 to 5). It is apparent that results from this study agree well with those of Belin et al.[8] and Brown.[6] The seemingly different results obtained by Gellings et al.[7] were the outcome of their unique selection of the axis, as discussed earlier in the introduction. The refined atomic positions obtained from this study have also been compared with the published data. As shown in Table 1, the results of the current study agree well with those of Belin et al.[8]. Brown[6] made obvious typographical errors in Zn(0) and Fe locations. Brown's designation of the y coordinate of the Zn(1) position was also inaccurate.

3.2 Results of the Atomistic Calculation

The cohesive energies of simple structures have been computed using ab initio methods. The computation results were then used to deduce the interatomic pair potentials using the lattice inversion technique. The pair potentials were, in turn, used to evaluate the cohesive energy of the $FeZn_{13}$ structure. The initial structure of $FeZn_{13}$ was constructed using Accelrys Cerius2 modeling software based on the atomic positions and lattice parameters determined experimentally. The structure was then refined using the energy minimization method with a potential cut-off radius of 1.4 nm. To avoid statistic fluctuation, a supercell $Fe_{16}Zn_{208}$ was applied to evaluate the lattice parameters and the cohesive energy. The calculated results are shown in Table 1 (column 6) with the errors indicated in parentheses. It can be seen that the calculated lattice constants and atom coordinates are consistent with the experimental results. The errors for lattice constants were less than 4.35%.

Global deformations, such as tension, compression, and shear, were applied to the proposed lattice in a computer simulation to check the stability of the calculated structures. Initial lattice constants of $FeZn_{13}$ were chosen arbitrarily in a certain range. Energy minimization was then applied to relax the system under the action of the potentials. It is shown in Table 2 that the final relaxed structure always converged to the same values regardless of the selection of initial values. It was demonstrated that the computation using the quasi-ab initio interatomic potentials was a reliable method to evaluate the lattice parameters and atomic coordinates.

Based on the *C*2/*m* structure of $FeZn_{13}$ and the interatomic potentials, the site preference of Fe and Zn in the narrow solubility range of $FeZn_{13}$ was studied. In each simulation, a certain number of Fe atoms were replaced by Zn atoms or a certain number of Zn atoms at a specific site were replaced by Fe atoms. The energy minimization method was then applied to relax the modified system under the action of the potentials. The stability of the modified structure was evaluated by energy and tolerance. The tolerance, which is the averaged result of 20 tests, represents the distortion of the atomic position from the initial space group.[13] The larger the tolerance, the more difficult it is for $FeZn_{13}$ to retain the initial space group. As shown in Fig. 4(a), the cohesive energy decreased with the number of

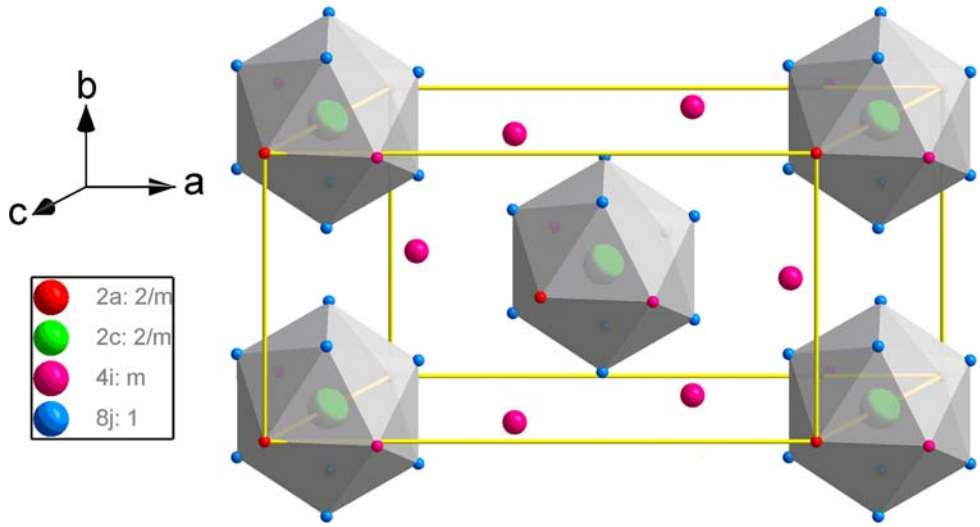

Fig. 3 Schematic illustration of the $FeZn_{13}$ lattice

Table 2 Determination of the lattice parameters of $FeZn_{13}$

Initial lattice parameter (unrelaxed)						Final lattice parameter (relaxed)						
a, nm	*b*, nm	*c*, nm	α	β	γ	*a*, nm	*b*, nm	*c*, nm	α	β	γ	Space group
1.5	0.8	0.6	90	128.92	90	1.3327	0.7478	0.5295	90	129.03	90	*C*2/*m*
1.0	0.6	0.5	90	128.92	90	1.3327	0.7478	0.5295	90	129.03	90	*C*2/*m*
1.328	0.749	0.528	90	150	90	1.3327	0.7478	0.5295	90	129.03	90	*C*2/*m*
1.328	0.749	0.528	90	45	90	1.3327	0.7478	0.5295	90	129.03	90	*C*2/*m*
1.3	0.7	0.6	90	90	90	1.3327	0.7478	0.5295	90	129.03	90	*C*2/*m*
1.2	0.8	0.4	90	90	90	1.3327	0.7478	0.5295	90	129.03	90	*C*2/*m*
1.1	0.9	0.3	90	120	90	1.3327	0.7478	0.5295	90	129.03	90	*C*2/*m*

substituted atoms, indicating that the $FeZn_{13}$ could become more stable after substitution. However, substitutions caused increases in tolerance, as revealed in Fig. 4(b), especially that of Zn atoms by Fe atoms at all Zn sites. This result indicated that the substitution of Zn by Fe was an impossible event, which is in convergence with the fact that the iron-rich phase boundary of the phase show no temperature and be at the ideal stoichiometry. On the other hand, substitutions of Fe by Zn atoms were allowed to a certain degree. The solubility range of $FeZn_{13}$ was reported to be 5.9 to 7.1 at.% Fe,[17] deviating from the nominal composition of 7.14 at.% Fe. Such a solubility range translated into the substitution of up to three atoms of Fe by Zn in an $Fe_{16}Zn_{208}$ super cell.

The possibility of Fe atoms occupying 2a positions and Zn atoms occupying 2c positions was explored computationally. It was found that the cohesive energy for Fe at the 2c position at ground state is lower than the proposed alternative by −3.5239 eV/atom. It was apparent that the most stable state was achieved when Fe atoms were located at 2c positions.

4. Conclusions

The lattice structure of $FeZn_{13}$ was determined experimentally. The space group for $FeZn_{13}$ is *C*2/*m* and the lattice parameters are $a = 1.34077(5)$ nm, $b = 0.76050(3)$ nm, $c = 0.50742(2)$ nm, and $\beta = 127.206(1)°$. The Fe atoms are located at the 2c position (0, 0, 0.5) and the coordinates for the Zn atom at the Zn(1) position are (0.114, 0.5, 0.293).

The structure of $FeZn_{13}$ was evaluated using a series of interatomic potentials obtained using the lattice inversion method. The results showed that the most stable state was achieved when Fe atoms located at the 2c positions, which was consistent with present experimental work. In the narrow solubility range for $FeZn_{13}$, Fe atoms are replaced by Zn atoms and Zn atoms cannot be replaced by Fe inverse, which indicates that the iron-rich phase boundary of the phase show no temperature and be at the ideal stoichiometry. In addition, the global deformations showed that the interatomic potentials were a reliable means of describing the structural properties of the $FeZn_{13}$ intermetallic.

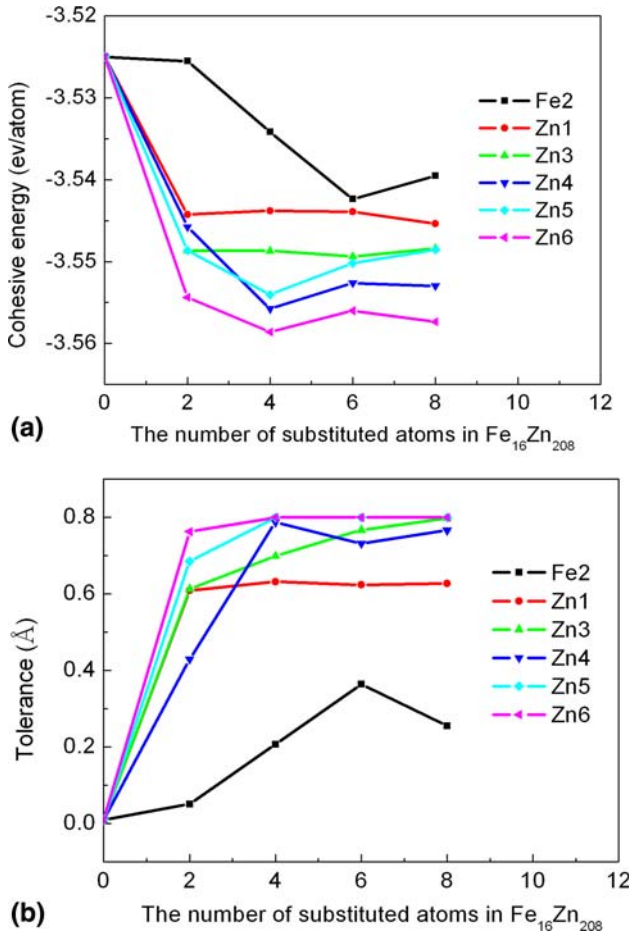

Fig. 4 The energy (eV/atom) (a) and the tolerance (b) variation with the content x of substituted atoms in a periodical cell, $Fe_{16}Zn_{208}$

The detailed description for the crystal structure of $FeZn_{13}$ is the fundamental for studying the solubility and site preference of alloying elements in $FeZn_{13}$, which is of great use to investigate the mechanism of Sandelin effect in further.

Acknowledgments

The authors would like to thank Prof. N.X. Chen at Tsinghua University and Prof. G.H. Rao and Dr. G.Y. Liu at the Institute of Physics in the Chinese Academy of Sciences for constructive discussions and encouragement. This work is supported by the National Natural Science Foundation of China (No. 50671088) and by the program for New Century Excellent Talents in Universities (NCET-04-778).

References

1. H. Guttman and P. Niessen, Reactivity of Silicon-Steels in Hot Dip Galvanizing, *Can. Metall. Q.*, 1972, **11**, p 609
2. L.P. Devillers, H. Guttman, and P. Niessen, The Mechanism of Excessive Coating Growth on Silicon Steels in Hot-dip Galvanizing, *Proceedings of Galvanization of Si Containing Steels*, ILZRO, Publ. Liege, 1975, **75**, p 48
3. X.P. Su, N.-Y. Tang, and J. Toguri, 450°C Isothermal Section of the Fe-Zn-Si Ternary Phase Diagram, *Can. Metall. Q.*, 2001, **40**(3), p 377
4. R.W. Sandelin, Galvanizing Characteristics of Different Types of Steels, *Wire Wire Prod.*, 1940, **15**, p 3
5. F. Götzl, F. Halla, and J. Schramm, δ_1 and ζ Phases in the Systems Fe-Zn and Co-Zn, *Z. Metallkd.*, 1941, **33**, p 375
6. P.J. Brown, The Structure of the ζ-Phase in the Transition Metal-Zinc Alloy Systems, *Acta Cryst.*, 1962, **15**, p 606
7. P.J. Gellings, E. Willam, and G. Gierman, Synthesis and Characterization of Homogeneous Intermetallic Fe-Zn Compounds, *Z. Metallkd.*, 1979, **70**, p 315
8. R. Belin, M. Tillard, and L. Monconduit, Redetermination of the Iron-Zinc Phase $FeZn_{13}$, *Acta Cryst. C*, 2000, **56**, p 267
9. N.X. Chen, J. Shen, and X.P. Su, Theoretical Study on the Phase Stability, Site Preference, and Lattice Parameters for $Gd(Fe,T)_{12}$, *J. Phys. Condens. Matter*, 2001, **13**, p 2727
10. N.X. Chen, Modified Möbius Inverse Formula and Its Applications in Physics, *Phys. Rev. Lett.*, 1990, **64**, p 1193
11. N.X. Chen, Z.D. Chen, and Y.C. Wei, Multidimensional Inverse Lattice Problem and a Uniformly Sampled Arithmetic Fourier Transform, *Phys. Rev. E*, 1997, **55**, p 5
12. N.X. Chen, S.Q. Hao, and Y. Wu, Phase Stability and Site Preference of $Sm(Fe,T)_{12}$, *J. Magn. Magn. Mater.*, 2001, **233**, p 169
13. H. Chang, N.X. Chen, J.K. Liang, and G.H. Rao, Theoretical Study of Phase Forming of $NaZn_{13}$-Type Rare-Earth Intermetallics, *J. Phys. Condens. Matter*, 2003, **15**(2), p 109
14. J.Y. Xie, N.X. Chen, J. Shen, L.D. Teng, and S. Seetharaman, Atomistic Study on the Structure and Thermodynamic Properties of Cr_7C_3, Mn_7C_3, Fe_7C_3, *Acta Mater.*, 2005, **53**, p 2727
15. J.C.P.D.S.—International Center for Diffraction Data, publishers of the Power Diffraction File, Newtown Square, PA
16. J. Rodriguez-Carvajal, *FULLPROF2000*, version July 2001, LLB, France, 2001
17. B.P. Burton, P. Perrot, and H. Okamoto, *Phase Diagrams 63 of Binary Iron Alloys*, H. Okamoto, Ed., 1993, p 459-466